Population Pharmacokinetics of Ibrutinib and Its Dihydrodiol Metabolite in Patients with Lymphoid Malignancies

Fanny Gallais, Loic Ysebaert, Fabien Despas, Sandra de Barros, Loïc Dupré, Anne Quillet-Mary, Caroline Protin, Fabienne Thomas, Lucie Obéric, Ben Allal, et al.

Clinical Pharmacokinetics
https://doi.org/10.1007/s40262-020-00884-0

ORIGINAL RESEARCH ARTICLE

Population Pharmacokinetics of Ibrutinib and Its Dihydrodiol Metabolite in Patients with Lymphoid Malignancies

Fanny Gallais[1] · Loïc Ysebaert[1,2] · Fabien Despas[3] · Sandra De Barros[4] · Loïc Dupré[5] · Anne Quillet-Mary[1] · Caroline Protin[2] · Fabienne Thomas[1,6] · Lucie Obéric[2] · Ben Allal[1,6] · Etienne Chatelut[1,6] · Mélanie White-Koning[1]

Abstract

Background and Objective Ibrutinib is used for the treatment of chronic lymphocytic leukemia and other lymphoid malignancies. The aim of this work is to develop a population pharmacokinetic model for ibrutinib and its dihydrodiol metabolite to quantify pharmacokinetic inter- and intra-individual variability, to evaluate the impact of several covariates on ibrutinib pharmacokinetic parameters, and to examine the relationship between exposure and clinical outcome.

Methods Patients treated with ibrutinib were included in the study and followed up for 2 years. Pharmacokinetic blood samples were taken from months 1 to 12 after inclusion. Ibrutinib and dihydrodiol-ibrutinib concentrations were assessed using ultra-performance liquid chromatography tandem mass spectrometry. A population pharmacokinetic model was developed using NONMEM version 7.4.

Results A total of 89 patients and 1501 plasma concentrations were included in the pharmacokinetic analysis. The best model consisted in two compartments for each molecule. Absorption was described by a sequential zero first-order process and a lag time. Ibrutinib was either metabolised into dihydrodiol-ibrutinib or excreted through other elimination routes. A link between the dosing compartment and the dihydrodiol-ibrutinib central compartment was added to assess for high first-pass hepatic metabolism. Ibrutinib clearance had 67% and 47% inter- and intra-individual variability, respectively, while dihydrodiol-ibrutinib clearance had 51% and 26% inter- and intra-individual variability, respectively. Observed ibrutinib exposure is significantly higher in patients carrying one copy of the cytochrome P450 3A4*22 variant (1167 ng.h/mL vs 743 ng.h/mL, respectively, $p = 0.024$). However, no covariates with a clinically relevant effect on ibrutinib or dihydrodiol-ibrutinib exposure were identified in the PK model. An external evaluation of the model was performed. Clinical outcome was expressed as the continuation or discontinuation of ibrutinib therapy 1 year after treatment initiation. Patients who had treatment discontinuation because of toxicity had significantly higher ibrutinib area under the curve ($p = 0.047$). No association was found between cessation of therapy due to disease progression and ibrutinib area under the curve in patients with chronic lymphocytic leukemia. For the seven patients with mantle cell lymphoma studied, an association trend was observed between disease progression and low exposure to ibrutinib.

Conclusions We present the first population pharmacokinetic model describing ibrutinib and dihydrodiol-ibrutinib concentrations simultaneously. Large inter-individual variability and substantial intra-individual variability were estimated and could not be explained by any covariate. Higher plasma exposure to ibrutinib is associated with cessation of therapy due to the occurrence of adverse events within the first year of treatment. The association between disease progression and ibrutinib exposure in patients with mantle cell lymphoma should be further investigated.

Trial Registration ClinicalTrials.gov no. NCT02824159.

1 Introduction

Ibrutinib (Imbruvica®) is a targeted therapy first approved by the US Food and Drug Administration in 2013. It is now used for the treatment of various B-cell malignancies such as chronic lymphocytic leukemia (CLL), mantle cell lymphoma (MCL) and Waldenström's macroglobulinemia

Electronic supplementary material The online version of this article (https://doi.org/10.1007/s40262-020-00884-0) contains supplementary material, which is available to authorized users.

✉ Loïc Ysebaert
ysebaert.loic@iuct-oncopole.fr

Extended author information available on the last page of the article

Published online: 24 April 2020

Key Points

For the first time, a population pharmacokinetic model for ibrutinib and its dihydrodiol metabolite in a real-life population of patients was developed.

The final model was complex, linear and showed large inter- and intra-individual variability.

Higher plasma exposure to ibrutinib was associated with cessation of ibrutinib therapy for toxicity within the first year of treatment.

(WM) [1]. Ibrutinib was developed as a selective and irreversible inhibitor of the Bruton tyrosine kinase (BTK) [2], a non-receptor protein kinase that plays a central role in the B-cell antigen receptor (BCR) pathway. The BCR signaling pathway is crucial for the development and survival of B cells as it is involved in the regulation of their proliferation, differentiation, migration and apoptosis [3]. The BCR has been shown to be involved in various B-cell malignancies [4] and given the essential role of BTK in this pathway, it has been investigated as a target for the treatment of these diseases [5]. Ibrutinib binds covalently to BTK cysteine-481 amino acid, leading to the irreversible inhibition of BTK phosphorylation and enzymatic activity, and therefore alters the BCR signaling cascade. The inhibition of BTK activity by ibrutinib is associated with several anti-leukemic effects on the lymphocytes including inhibition of proliferation, egress from lymph nodes (tumoral niches), inhibition of re-homing to niches, and death in blood and niches [6, 7].

This work focuses on the study of ibrutinib pharmacokinetics. Ibrutinib is an oral drug administered once a day. The standard posology is 420 mg for CLL and WM and 560 mg for MCL. Ibrutinib is predominantly metabolised in the liver by the cytochrome P450 (CYP) 3A family members CYP3A4 and CYP3A5 [8]. Its oral bioavailability is very poor ($F = 2.9\%$; 90% confidence interval 2.1–3.9) owing to high first-pass hepatic metabolism [8, 9]. One of its active metabolites, dihydrodiol-ibrutinib (DHD-ibrutinib), is about 15 times less active than ibrutinib [10] but exhibits lower plasma protein binding (91% binding compared with 97% for ibrutinib) and has concentrations up to twice those of ibrutinib. No specific clinical activity or particular toxicity related to DHD-ibrutinib is known.

The pharmacokinetics of ibrutinib is highly variable in patients. If a relationship between drug exposure and toxicity or efficacy exists, therapeutic drug monitoring (TDM) would be beneficial for patients treated with ibrutinib. A first population pharmacokinetic (popPK) model for ibrutinib was proposed by Marostica et al. [11]. This model was built based on the data collected in three phase I and phase II clinical studies, but did not include data pertaining to metabolites. The objective of our work is to develop a new popPK model considering ibrutinib and its metabolite simultaneously based on real-life patient population data. The aim of this model is to describe the concentrations of both molecules, to quantify pharmacokinetic (PK) inter- and intra-individual variability, to evaluate the impact of several covariates on ibrutinib PK parameters in a population of patients treated with ibrutinib, to analyse the relationship between exposure to ibrutinib and response to treatment, and to discuss the potential benefit of TDM for ibrutinib.

2 Methods

2.1 Study Population

The subjects in this analysis include those in the ibrutinib cohort of the PK-E3i study, which was initiated within the hematology department of IUCT-Oncopole hospital (Toulouse, France) in 2016. PK-E3i is an observational PK-pharmacodynamic (PD) study approved by the competent authority (ANSM, under No. 151668A-11) and the ethics committee (under No. CPP16-004a), registered by ClinicalTrials.gov under No. NCT02824159 and carried out by the university hospital of Toulouse. Patients treated by ibrutinib for CLL, MCL or WM were recruited from 2016 to 2018 and followed up for 2 years. All patients gave their written informed consent. Seven hospital visits were planned at months 1, 2, 3, 6, 12, 18 and 24 after inclusion (M1–M24 visits). Pharmacokinetic blood sampling was performed from M1 to M12. Ibrutinib was taken orally once daily at a starting dose of 420 mg (CLL, MW) or 560 mg (MCL). Because of the occurrence of adverse drug reactions, some patients subsequently had their dose reduced.

2.2 Data Collection

Rich PK blood sampling was performed at steady state during the M1 visit. A total of six blood samples were taken at $t = 0$ h (before drug administration) and 0.5, 1, 2, 4 and 6 h after administration. Single PK blood samples were collected at M2–M12 as before drug intake, to assess for trough concentrations. Samples were collected in heparinised lithium tubes of 5 mL. The tubes were centrifuged (1400 × g, room temperature, 10 minutes) and plasma was collected and frozen at – 20 °C until analysis. An ultra-performance liquid chromatography in tandem with a mass spectrometer (Waters, St Quentin en Yvelines, France) was used for method development and validation in our laboratory. The method was built for a robust simultaneous quantification of a panel of tyrosine kinase inhibitors including ibrutinib and DHD-ibrutinib. The lower limit of quantification was

0.98 ng/mL for both molecules. One saliva sample was collected for CYP3A4 and CYP3A5 genotyping at inclusion using a commercial kit (GeneFiX™ Saliva-Prep DNA Isolation kit). Based on previous work [12, 13], we focused our interest on CYP3A4*22 and CYP3A5*3, which are the main clinically relevant alleles of CYP3A4 and CYP3A5 associated with altered drug metabolism. The presence of CYP3A5*1/CYP3A5*3 alleles was determined on genomic DNA with allele-specific real-time polymerase chain reaction using melt curve analysis as previously described [14]. The CYP3A4*22 allele was genotyped using allelic discrimination with TaqMan assay (c_59013445_10) following the manufacturer's instructions.

2.3 Population-Pharmacokinetic Modelling

2.3.1 General Modelling Strategy

First, a popPK model for ibrutinib only was built. The structural model obtained for ibrutinib was then used to build a more complex model including the metabolite observations. Different methods of taking first-pass hepatic metabolism into account in the model were assessed. Inter-occasion variability was tested on all PK parameters considering one occasion for each hospital visit. Non-zero covariance terms were added in the OMEGA matrix to assess for correlations between ibrutinib and DHD-ibrutinib PK parameters. To ensure model stability, the covariate analysis was performed on the model with a diagonal OMEGA matrix. The final model was externally evaluated on an independent population of patients. Model development was performed with NONMEM version 7.4.1 (ICON Development Solutions, Ellicott City, MD, USA) using first-order conditional estimation with an interaction estimation method. Data management and graphical analyses were performed in R version 3.4.2.

2.3.2 Covariate Analysis

Morphological, biological and clinical covariates were selected from PK-E3i patient case report forms. Continuous covariates were added to the model in an allometric manner. Categorical covariates were added to the model in a multiplicative form. To assess for statistical significance of covariate effects, we performed a univariate analysis where all covariates were tested separately on the main PK parameters of interest: ibrutinib and DHD-ibrutinib elimination clearances (CL_{ibru}, CL_{DHD}), first-pass hepatic metabolism constant (KA_{DHD}) and ibrutinib to DHD-ibrutinib metabolism clearance (CL_{met}). Covariates were tested simultaneously on the last two parameters (one θ_{COV} estimation for both parameters) because it was assumed that they described the same physiological process (hepatic metabolism). Covariates associated with a decrease of objective function value (OFV) greater than 3.84 (Chi-squared test, $df = 1$, $p \leq 0.05$) and a decrease of interindividual variability greater than 1% were included in a multivariate model. Then covariates were removed one by one. Covariates associated with an increase of OFV greater than 6.6 (Chi-squared test, $df = 1$, $p = 0.01$) were kept in the model, others were definitively removed. This process was continued until only statistically significant covariates remained in the model. Multiple testing was accounted for by choosing low significance levels at each step of the covariate analysis (5% and 1% at the univariate and multivariable steps, respectively).

If a covariate (c) was missing at a visit (v) for patient i, the missing value was replaced by the value of c at the previous visit ($v - 1$). If no value was available at the previous visit, the missing value was replaced by the population median of c at visit v.

2.3.3 Model Evaluation

Model selection and evaluation was based on OFV value, goodness-of-fit plots, residual variability estimates, relative standard errors, stability of the estimates and shrinkage values. The model was externally evaluated on a second population that was independent from the model development population but similar to it. The second population consisted of 28 patients receiving treatment at the IUCT-Oncopole Hospital Hematology Department between 2014 and 2016. At the request of the prescribing clinician and to carefully monitor treatment, PK data were routinely collected at each hospital visit. Patient blood samples were collected for one PK exploration at steady state before drug administration and 0.5, 1, 2, 4 and 6 h after administration.

To perform the external evaluation of our model, all parameters were fixed to their estimated value and the NONMEM option MAXEVAL = 0 in the $ESTIMATION section was used. Median prediction error (%) [bias] and median absolute prediction error (%) [inaccuracy] were calculated. The prediction error (PE) is defined as $\mathrm{PE} = \frac{C_{pred} - C_{obs}}{C_{obs}} \times 100$ where C_{pred} is the predicted concentration and C_{obs} is the observed concentration [15]. In addition, we calculated the percentage of absolute PEs inferior to 20% and 30% (F_{20} and F_{30}, respectively). Visual predictive checks were also used to assess for predictive performance of the model.

2.4 Pharmacokinetic-Pharmacodynamic Evaluation

The PK-E3i study is currently on-going with some of the patients still being monitored. As a preliminary PK-PD analysis, the relationship between pharmacokinetics and

continuation of ibrutinib therapy 1 year after treatment initiation was explored. We looked at the association between ibrutinib area under the curve (AUC) and clearance at the M1 visit and whether the patients had their treatment discontinued because of toxicity or a lack of efficacy or if it was continued 1 year after inclusion.

3 Results

A total of 93 patients were included in the study. Four were withdrawn from the study before the M1 visit and therefore unable to perform a plasma drug determination because of refusal to participate ($n = 1$), disease progression ($n = 2$) or death ($n = 1$). Therefore, a total of 89 patients and 1501 concentrations (including ibrutinib and DHD-ibrutinib) were used in the model development. Of these, 27 (30%) were women and 62 (70%) were men, with a mean age of 69 years (range: 31–84 years). Patients were treated for CLL (87%), MCL (11%) or WM (2%). Detailed information about patients' characteristics can be found in Table 1. Drug concentrations under the lower limit of quantification (4%) were considered equal to the lower limit of quantification/2 = 0.49 ng/mL. Concentrations over time profiles according to the dose received are represented in Fig. 1. Although variability is very important, Fig. 1 shows that plasmatic ibrutinib and DHD-ibrutinib concentrations increase as the dose is increased.

3.1 Step 1: Ibrutinib Population-Pharmacokinetic Model

First, a popPK model was built for ibrutinib. A model with two compartments was found to best describe the data. Several absorption models were tested. The best

Table 1 Patient covariates at baseline ($n = 89$)

Characteristics	Mean [range]	Characteristics	Mean [range]
Age (years)	69 [31–84]	$CD4^+$ T cells (/mm^3)	1682 [1034–7571]
Height (cm)	169 [146–189]	$CD8^+$ T cells (/mm^3)	1296 [66–6814]
Weight (kg)	73 [40–113]	CrCL (mL/min)	64 [27–81]
BMI (kg/m^2)	25.5 [16.6–36.3]	Total bilirubin (μmol/L)	13 [4–228]
BSA (m^2)	1.8 [1.3–2.4]	GGT (g/L)	6.4 [1.2–28.0]
Lymphocytes (g/L)	101.6 [0.3–430]	LDH (UI/L)	276 [108–892]
Neutrophils (g/L)	4.3 [2.0–14.0]	ALT (UI/L)	30 [11–109]
Platelets (g/L)	141.2 [7.0–343.0]	AST (UI/L)	26 [9–71]
Hemoglobin (g/dL)	11.0 [3.6–16.0]		
Characteristics	**Number (%)**	**Characteristics**	**Number (%)**
Sex		CYP3A4 genotype	
Female	27 (30)	*1/*1	80 (90)
Male	62 (70)	*1/*22	9 (10)
Disease			
CLL	77 (87)	CYP3A5 genotype	
MCL	10 (11)	*3/*3	84 (14)
WM	2 (3)	*1/*3	5 (6)
Prior treatment		Smoking	
Yes	70 (79)	Yes	18 (20)
No	19 (21)	No	71 (80)
Performance status		Alcohol consumption	
0	22 (25)	Yes	9 (10)
1	51 (57)	No	80 (90)
2	16 (18)		
Coadministration with antacids			
Yes	26 (29)		
No	63 (71)		

ALT alanine aminotransferase, *AST* aspartate aminotransferase, *BMI* body mass index, *BSA* body surface area, *CLL* chronic lymphocytic leukemia, *CrCL* creatinine clearance, *CYP* cytochrome P450, *GGT* gamma globulins total, *LDH* lactate dehydrogenase, *MCL* mantle cell lymphoma, *WM* Waldenström's macroglobulinemia

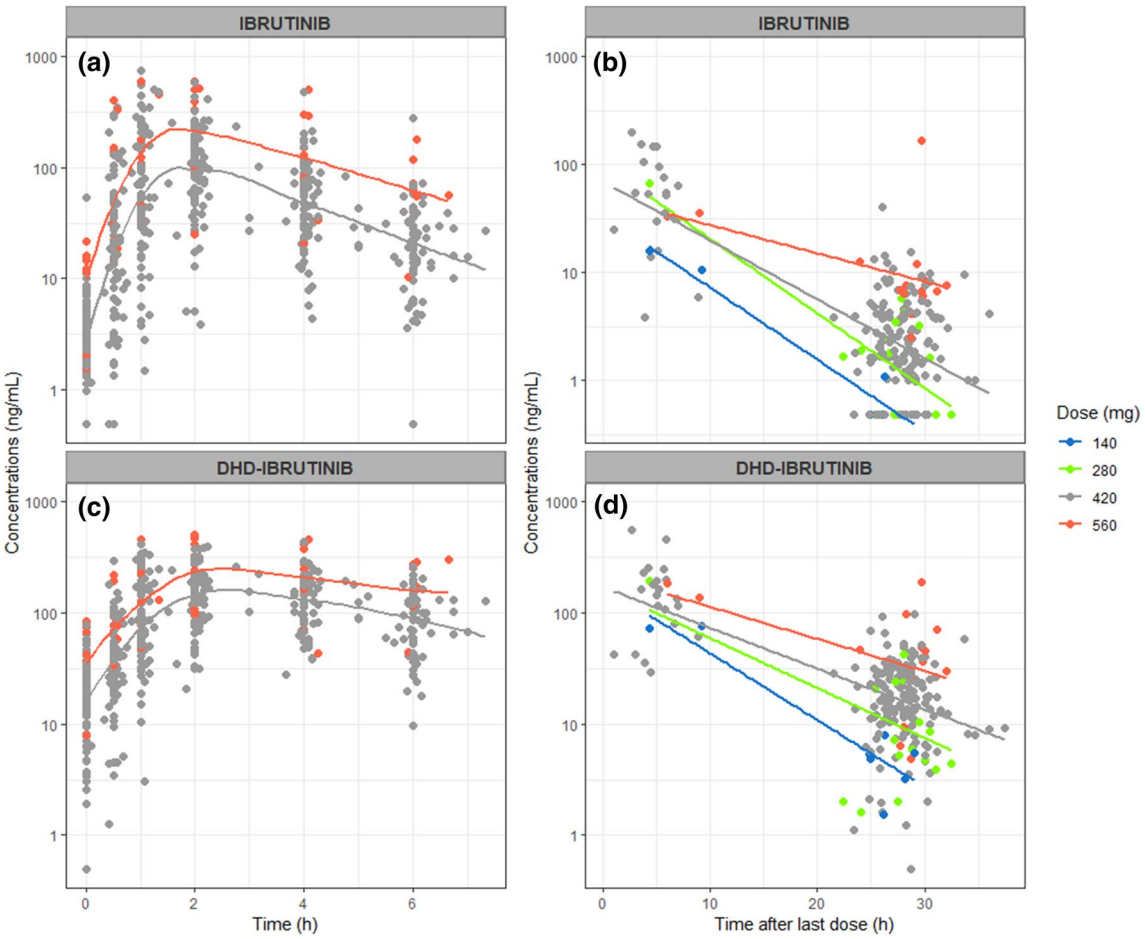

Fig. 1 Observed concentrations of ibrutinib (**a**, **b**) and dihydrodiol-ibrutinib (**c**, **d**) according to dose. Figures (**a**) and (**c**) represent the data obtained with rich sampling (six samples from 0 to 6 hours after administration) at the M1 visit (1 month after inclusion and treatment initiation). Figures (**b**) and (**d**) represent concentrations obtained from a single sample taken before drug administration at M2, M3 and M6 visits (2, 3 and 6 months after inclusion, respectively)

absorption model was a sequential zero-first absorption with a lag time. Bioavailability was fixed to the value $F1 = 3\%$ [10] and inter-individual variability was estimated on $F1$. This last step was found to improve the model performances significantly (drop in OFV over 100 points). A schematic of the final popPK model for ibrutinib is available in the Electronic Supplementary Material (ESM).

3.2 Step 2: Ibrutinib and Dihydrodiol-Ibrutinib Population-Pharmacokinetic Model

The global structure of the model obtained in step 1 was kept for ibrutinib. As demonstrated in step 1 by the need to add the bioavailability parameter $F1$ in the model, a crucial question was how to take into account first-pass hepatic metabolism in the model to obtain a good description of the observed data. Dihydrodiol-ibrutinib volumes of distribution were fixed as equal to those of ibrutinib as the metabolised fraction was unknown and hence the metabolite volume of distribution could not be estimated. Finally, the best model (Fig. 2) consisted of one dosing compartment, two compartments for both ibrutinib and DHD-ibrutinib. Absorption was described by a lag time (ALAG1) and a sequential zero first-order process (D1, KA_{ibru}). Ibrutinib can be either metabolised into DHD-ibrutinib (CL_{met}) or excreted through other routes of elimination (CL_{ibru}). Dihydrodiol-ibrutinib is then eliminated (CL_{DHD}). A link between the dosing compartment and the DHD-ibrutinib central compartment was added to assess for high first-pass hepatic metabolism (KA_{DHD}). Non-zero covariance terms in the omega matrix were found to improve the model (the detailed OMEGA matrix can be found in the ESM). Proportional residual variability was estimated for ibrutinib (σ_{ibru}) and DHD-ibrutinib (σ_{DHD}). Inter-occasion variability was estimated for both ibrutinib and DHD-ibrutinib elimination clearances.

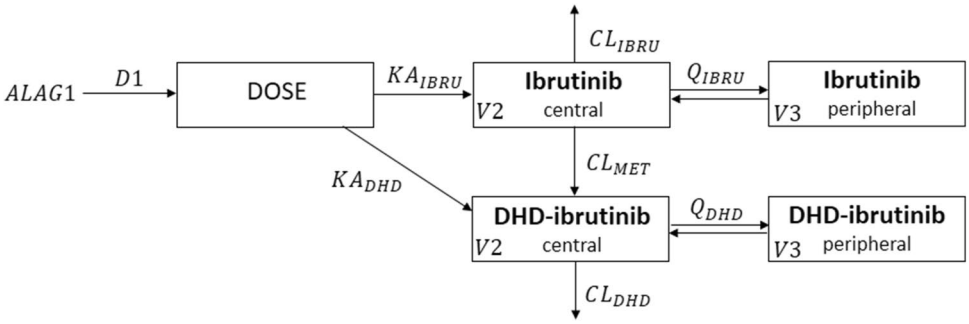

Fig. 2 Final population pharmacokinetic model for ibrutinib and its dihydrodiol (DHD) metabolite. Absorption is delayed with a lag time (ALAG1) and is modelled by a zero first-order sequential process with parameters $D1$ and KA_{ibru} for zero and first-order process, respectively. First-pass hepatic metabolism is modelled by a link between the dosing compartment and metabolite central compartment with parameter KA_{DHD}. Both molecules have a distribution compartment. Dihydrodiol–ibrutinib volumes of distribution were fixed to the same values as those of ibrutinib: V2 is the central volume of distribution and V3 is the peripheral volume of distribution. Ibrutinib can be either metabolised into DHD-ibrutinib (CL_{met}) or excreted through other routes of elimination (CL_{ibru}). Dihydrodiol-ibrutinib is then eliminated (CL_{DHD}). All clearance and volume parameters are apparent

3.3 Step 3: Covariate Analysis

All tested covariates are summarised in Table 1. A univariate analysis led to the selection of the following covariates: CD4 + T cells, prior treatment and performance status on CL_{ibru}, CYP3A4*22 genotype on CL_{DHD}, and body mass index on KA_{DHD} and CL_{met}, with $CD4^+$ T-cell count and body mass index being time-varying covariates (the value for each visit was used in the analysis). These covariates were then included in the multivariate analysis. Finally, none of the tested covariates had a significant statistical impact in the model ($p = 0.01$). Ibrutinib and DHD-ibrutinib AUC were simulated for virtual patients with each covariate varying from its 10th to its 90th percentile (while all other covariates were fixed to their typical value) [16]. Ibrutinib AUC was calculated using model parameters as follows:

$$AUC_{ibru} = \frac{DOSE \times \left(\frac{KA_{ibru}}{KA_{DHD}+KA_{ibru}}\right)}{CL_{met} + CL_{ibru}},$$

whereas DHD-ibrutinib AUC was calculated using the trapezoidal method with the population concentrations predicted by the model. Results are summarised in Fig. 3. None of the tested covariates led to a change of AUC greater than 30% except for the CYP3A4 genotype on CL_{DHD}, which led to a 38% increase of DHD-ibrutinib AUC. Regarding this last result, the relationship between observed ibrutinib and DHD-ibrutinib AUC and CYP3A4/5 genotypes was evaluated: patients carrying the CYP3A4*22 variant associated with lower metabolic activity had mean observed ibrutinib and DHD-ibrutinib AUC 1.6-fold higher (1167 ng.h/mL vs 743 ng.h/mL) and 1.5-fold higher (2597 ng.h/mL vs 1777 ng.h/mL) than in the reference group, respectively. These associations were statistically significant (Wilcoxon test: $p = 0.024$ for ibrutinib and $p = 0.028$ for DHD-ibrutinib). No significant association was found for CYP3A5*3. Concerning the potential dose–concentration relationship, no systematical decrease or increase of clearance values over time was observed. Percentage of clearance variation compared to occasion 1 was randomly distributed with a median close to 0% for both molecules. Final model parameter estimations are presented in Table 2. Goodness-of-fit plots are shown in Fig. 4.

3.4 Step 4: External Evaluation of the Model

The model represented in Fig. 2 was externally evaluated. A total of 28 additional patients and 352 concentrations were included in the analysis. This independent population was similar to the main population as it consisted of 11 (39%) women and 17 (61%) men, with a mean age of 69 years, treated with ibrutinib for CLL (86%) or MCL (14%). Median prediction error and median absolute prediction error were calculated with individual- and population-predicted concentrations for ibrutinib and DHD-ibrutinib (Fig. 5). According to individual model predictions, predictive performances are very satisfactory. Bias is less than 10% for ibrutinib and less than 5% for DHD-ibrutinib. Inaccuracy is less than 20% for ibrutinib and less than 15% for DHD-ibrutinib. Prediction-corrected visual predictive checks are good. For population predictions, bias values remain satisfactory (less than 10%) but predictions are not very accurate (around 50% and 40% imprecision for ibrutinib and DHD-ibrutinib respectively), only 23% of ibrutinib concentrations and 41% of DHD-ibrutinib concentrations are well predicted (PE < 30%).

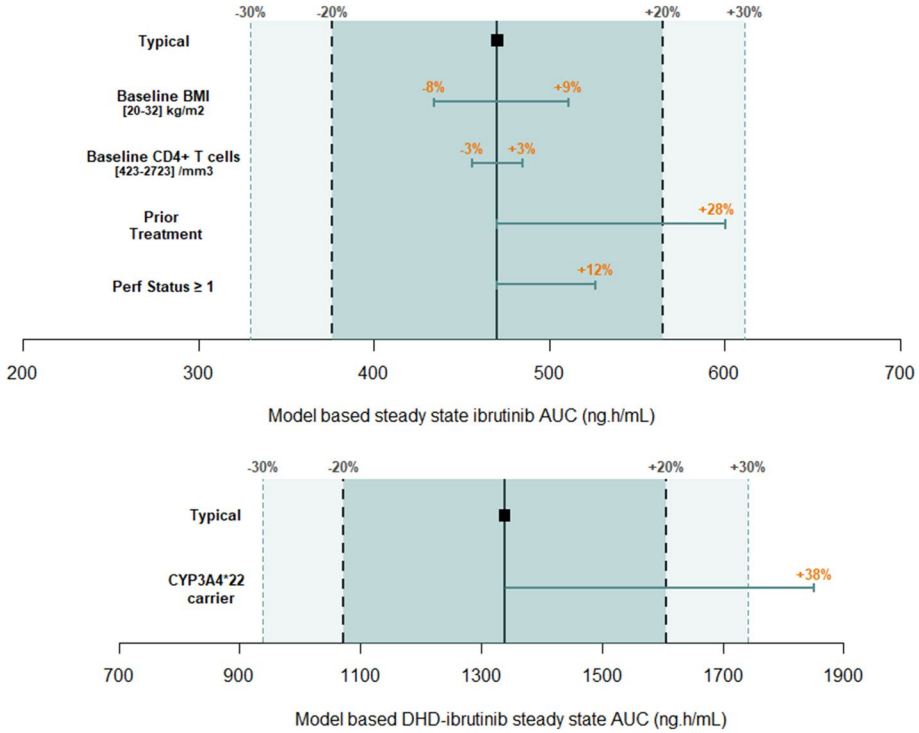

Fig. 3 Evaluation of the impact of significant covariates in a univariate analysis on ibrutinib and dihydrodiol (DHD)-ibrutinib area under the curves (AUCs). The solid black vertical line is the AUC for a typical patient. Dotted black lines correspond to variations of AUC of 20% and 30%. Blue horizontal bars represent a change in the AUC for the corresponding covariate varying from its 10th to its 90th percentile. Percentage changes in AUCs are written in orange

Table 2 Parameter estimates for the final ibrutinib and dihydrodiol-ibrutinib population pharmacokinetic model

Parameters	Estimation (RSE)	Interindividual variability CV% (RSE) [shrinkage]	Inter-occasion variability CV% (RSE) [shrinkage]
ALAG1(h)	0.238 (16%)	80.6% (16%) [16%]	NE
$D1$(h)	0.989 (19%)	115.2% (16%) [12%]	NE
$\mathrm{KA}_{\mathrm{ibru}}\left(\mathrm{h}^{-1}\right)$	1.56 (18%)	NE	NE
$\mathrm{KA}^{\mathrm{a}}_{\mathrm{DHD}}(\mathrm{h}^{-1})$	1.21 (20%)	64.2% (24%) [4%]	NE
$\mathrm{CL}^{a}_{\mathrm{IBRU}}$(L/h)	242 (11%)	66.5% (24%) [2%]	46.7% (13%) [17%]
$V2^{a}$(L)	1010 (9%)	81.8% (19%) [1%]	NE
Q_{IBRU}(L/h)	171 (16%)	NE	NE
$V3^{a}$(L)	1480 (9%)	76.9% (20%) [4%]	NE
$\mathrm{CL}^{a}_{\mathrm{MET}}$(L/h)	150 (19%)	64.4% (21%) [12%]	NE
$\mathrm{CL}^{a}_{\mathrm{DHD}}$(L/h)	181 (9%)	50.7% (12%) [0%]	25.7% (8%) [23%]
Q_{DHD}(L/h)	50 (13%)	NE	NE
Proportional residual variability CV% (RSE) [shrinkage]			
σ_{IBRU}	37% (13%) [24%]		
σ_{DHD}	25.7% (8%) [25%]		

Variance-covariance matrix is available in the ESM. Proportional residual variability was 37% for ibrutinib and 25.7% for DHD-ibrutinib. All clearance and volume parameters are apparent

Interindividual variability was estimated for every parameter except KA_{ibru} and inter-compartmental clearances. Inter-occasion variability was estimated for both elimination clearances. Non-zero covariance terms were estimated between $D1$ and ALAG1, and between all parameters a

*ALAG*1 lag time for absorption, CL_{ibru} and CL_{DHD} ibrutinib's and DHD-ibrutinib's elimination clearances, CL_{met} ibrutinib's clearance of metabolisation into DHD-ibrutinib, *CV%* percentage coefficient of variation, *DHD* dihydrodiol, $D1$ and KA_{ibru}zero and first-order absorption parameters, KA_{DHD} FPHM parameter, Q_{ibru} and Q_{DHD} are inter-compartmental clearance for ibrutinib and DHD-ibrutinib, *RSE* relative standard error, $V2$ and $V3$ are central and peripheral volumes of distribution for both molecules

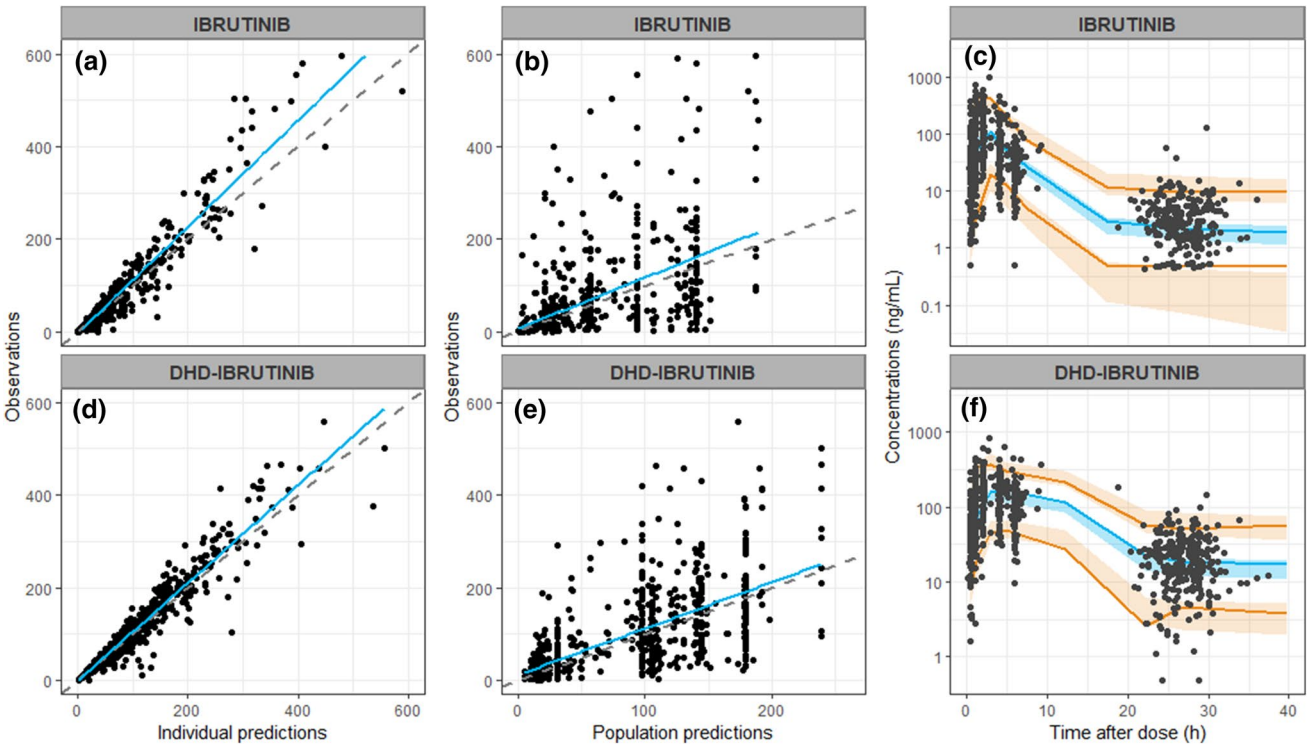

Fig. 4 Goodness-of-fit plots of the final population pharmacokinetic model for ibrutinib (**a**–**c**) and dihydrodiol (DHD)-ibrutinib (**d**–**f**). For observations vs individual predictions (**a**, **d**) and observations vs population predictions (**b**, **e**), the blue line is linear regression and the gray dotted line is the identity line. For prediction-corrected visual predictive checks [1000 simulations] (**c**, **f**), points are observed data, colored areas are the 5th (orange), 50th (blue) and 95th (orange) percentiles of simulated concentrations, whereas orange and blue lines are the 5th, 50th and 95th percentiles of observed concentrations

3.5 Pharmacokinetic-Pharmacodynamic Relationship

A preliminary analysis of the ibrutinib PK-PD relationship was performed. One year after inclusion, 66 patients were still receiving therapy, eight discontinued their treatment for toxicity, 11 for inefficacy (disease progression) and four for other reasons (refusal to participate in the study, progression of other disease and death from other cause). Patients who discontinued therapy because of the occurrence of an adverse drug reaction had a 1.5-fold higher mean ibrutinib AUC at visit M1 than patients who did not discontinue treatment (Fig. 6) [Wilcoxon test, $p = 0.048$]. In terms of efficacy, patients with CLL and MCL were distinguished (the WM population was ignored as it contained only two patients). In the CLL population, 62 patients were still receiving treatment at month 12, whereas six patients discontinued treatment because of disease progression. No difference was observed between the two groups in terms of exposure to ibrutinib at visit M1. In the MCL population, two patients were still receiving treatment at month 12, whereas five patients discontinued treatment because of disease progression. Patients with MCL who discontinued treatment had lower ibrutinib AUC (0.45-fold lower mean AUC) but this association was not statistically significant (Fig. 7).

4 Discussion

The popPK model we developed for ibrutinib is consistent with the model proposed by Marostica et al. [11]. Several methods of modelling the first-pass hepatic effect were investigated. The reproduction of the model developed by Lindauer et al. for sunitinib [17] was not possible as no information was available concerning the ibrutinib fraction metabolised into DHD-ibrutinib. A model similar to that presented by Yu et al. [18] was also tested, with two dosing compartments, one representing ibrutinib and one representing the metabolite, and initialisation with part of the dose. ter Heine et al. proposed a model with a liver compartment and hypothesised rapid equilibrium between the liver and parent central compartment [19]. These models were not selected because of the instability of parameter estimates and bad fit of the data. The model finally selected in our study was similar to that presented by Bertrand et al. [20] and Kerbusch et al. [21]. The simple addition of a link between

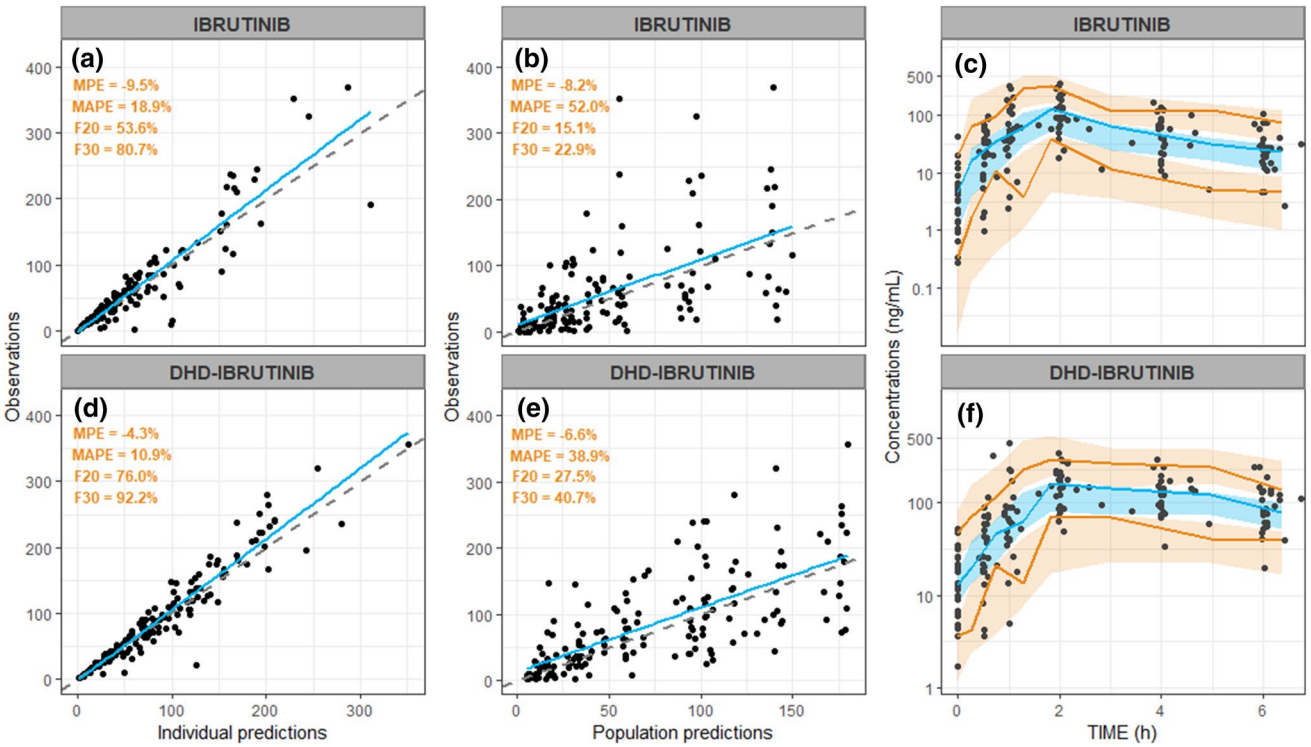

Fig. 5 External evaluation of the final population pharmacokinetic model for ibrutinib (**a**–**c**) and dihydrodiol (DHD)-ibrutinib (**d**–**f**). For observations vs individual predictions (**a**, **d**) and observations vs population predictions (**b**, **e**), the blue line is linear regression and the gray dotted line is the identity line. For prediction-corrected visual predictive checks [1000 simulations] (**c**, **f**), points are observed data, colored areas are the 5th (orange), 50th (blue) and 95th (orange) percentiles of simulated concentrations whereas orange and blue lines are the 5th, 50th and 95th percentiles of observed concentrations

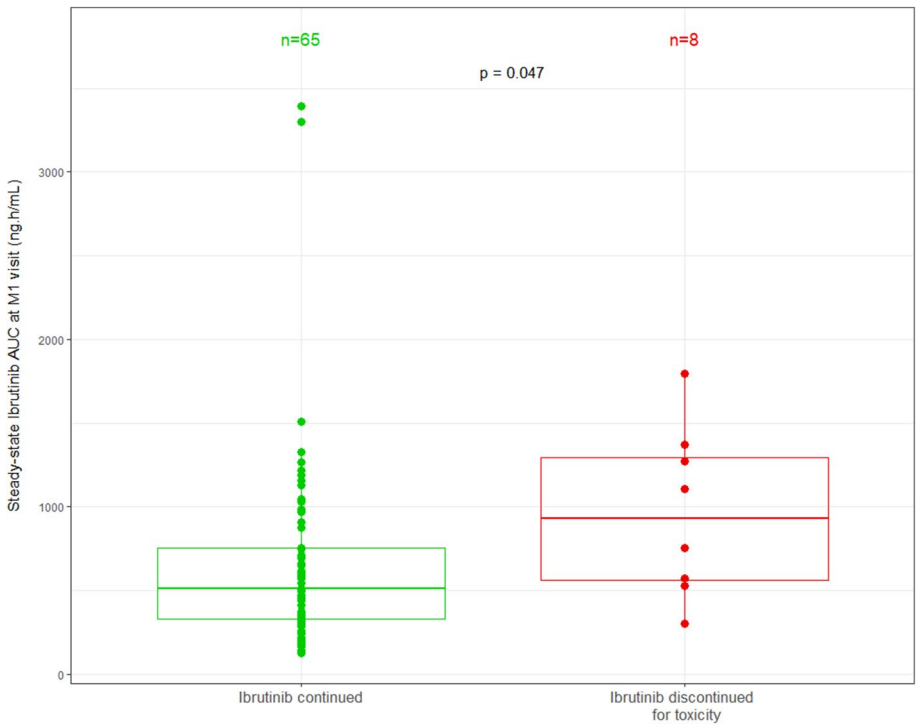

Fig. 6 Comparison of steady-state area under the curve (AUC) calculated from pharmacokinetic post-hoc parameters at hospital visit M1 between patients who discontinued ibrutinib within the first year of treatment because of the occurrence of an adverse event and patients who were still receiving therapy 1 year after inclusion. A statistically significant association was found: patients who underwent adverse events had higher ibrutinib AUC ($p = 0.048$)

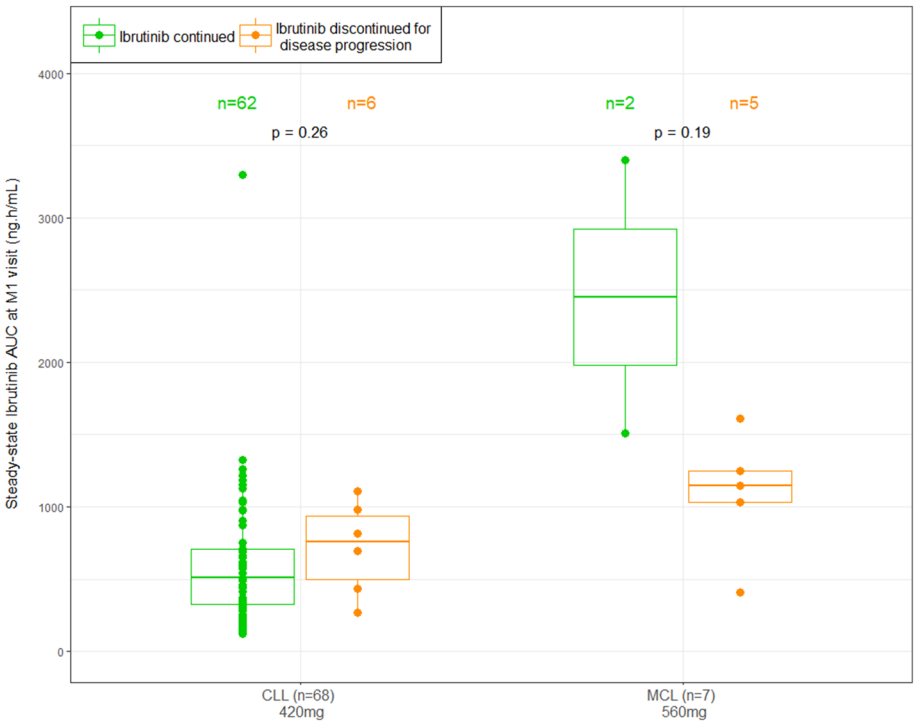

Fig. 7 Comparison of steady-state area under the curve (AUC) calculated from pharmacokinetic post-hoc parameters at hospital visit M1 between patients who discontinued ibrutinib within the first year of treatment because of disease progression and patients who were still receiving therapy 1 year after inclusion. Patients were separated according to their disease (chronic lymphocytic leukemia [CLL] or Mantle cell lymphoma [MCL]). No statistically significant association was observed for either of the two groups. A trend of under-exposure in patients who had disease progression was observed for patients with MCL indicating that this association should be further explored

the dosing compartment and the metabolite central compartment was sufficient to describe the first-pass hepatic effect. In their analysis, Marostica et al. showed a significant effect of food on bioavailability (decreased in the fasted condition) and on the absorption parameter $D1$ (increased in the fasted condition). These results could not be confirmed in our study as this covariate was not available for our population. The recommendation that ibrutinib should be taken 30 minutes before or 2 hours after food intake was explicitly given by the clinicians to the patients but there is no guarantee that they followed it, nor any data to assess it. Marostica et al. also found an effect of the coadministration of antacid drugs on $D1$ (increased in the presence of antacid comedications). This covariate was tested in our model but no statistically significant effect was found. However, in our study, the coadministration of antacids was only reported as "yes or no" the day of the hospital visit. As the time of antacid administration can vary, we may have missed a significant effect of antacid coadministration on ibrutinib concentrations. Furthermore, none of the tested covariates had a clinically relevant impact as none of them led to a change of AUC greater than 30% (except for the CYP3A4 genotype on CL_{DHD}, which led to a 38% increase of DHD-ibrutinib AUC). Intra-individual variability was also quantified in the final model. The estimations were large, around 50% and 30% for ibrutinib and DHD-ibrutinib clearance of elimination, respectively. As mentioned above, this intra-individual variability could partly be explained by food conditions. The final model was externally evaluated (Fig. 5). The results of the evaluation proved that our structural model is accurate, as both molecule bias and inaccuracy in individual predictions were under 10% and 20%, respectively. Inaccuracy in population predictions (median absolute prediction error) was around 50% for ibrutinib and 40% for DHD-ibrutinib, which implies that covariate identification is still needed to account for the interindividual variability.

Ibrutinib is extensively metabolised in the liver by CYP3A4 and to a lesser extent by CYP3A5. It has been shown that exposure to ibrutinib is lower or higher when administered with CYP3A inducers or inhibitors, respectively [9]. Based on previous work [12], we focused our interest on CYP3A4*22 and CYP3A5*3. CYP3A4*22 is found in 5.3% of the Caucasian population and is associated with a lower metabolic activity than wild-type genotype CYP3A4*1/*1. The CYP3A5*3 variant is carried by 83% of the Caucasian population and is associated with a lower metabolism than the wild-type allele CYP3A5*1 [12, 13]. We found that carrying the CYP3A5*3 variant had no effect on ibrutinib PK presence, which is in agreement with its low contribution to ibrutinib metabolism [8] but could also be due to the low number of heterozygous patients (only five patients had the CYP3A5*1/CYP3A5*3 genotype). For CYP3A4, nine patients had the CYP3A4*1/CYP3A4*22 genotype. Ibrutinib observed AUC was significantly higher in patients carrying one copy of the CYP3A4*22 allele ($p = 0.024$) but CYP3A4*22 was not a significant covariate for ibrutinib clearance in our model. Higher DHD-ibrutinib observed AUC was also found in patients carrying

CYP3A4*22 ($p = 0.027$). CYP3A4*22 was found to be a significant covariate impacting DHD-ibrutinib clearance in a univariate analysis and we showed through model simulations that the presence of CYP3A4*22 led to a 38% increase in DHD-ibrutinib steady-state AUC. These results suggest that DHD-ibrutinib is also metabolised through CYP3A4. This hypothesis was also mentioned in a previous study [10]. Regarding these results, the association between ibrutinib, DHD-ibrutinib exposure and CYP3A4 genotype status should be further investigated in larger populations to determine whether this information should be taken into account when choosing ibrutinib dosing.

Previous studies showed a decrease of BTK levels over time under ibrutinib treatment [22, 23]. Based on this observation and on the assumption that a stoichiometry law describes ibrutinib efficacy, Chen et al. conducted a pilot study in 11 patients with CLL to test the impact of reducing the ibrutinib daily dose as treatment progresses [24]. In their study, patients received three cycles of treatment from 420 mg/day (cycle 1), to 280 mg/day (cycle 2) and 140 mg/day (cycle 3). The authors observed globally similar plasmatic concentrations of ibrutinib and BTK occupancy during the three cycles, suggesting that reducing the dose of ibrutinib over time would have no impact on a patient's response to treatment. The same conclusion was reported in another study [25]. It is concordant with our results as we observed no trend between the progression group and the responding group, suggesting that the dose of 420 mg is above the required dose and that lowering it would not be associated with modification of the efficacy. Yet, while we do not question this conclusion, the assumption that a lower dose of ibrutinib will suffice to stoichiometrically inhibit BTK is in contradiction with our study and observed data. Such a phenomenon, which could be assimilated to the target-mediated drug disposition described for monoclonal antibody drugs, would be associated with a systematic decrease of ibrutinib clearance over time. In our population, no systematical decrease of clearance values over time was observed. Mean plasmatic ibrutinib and DHD-ibrutinib concentrations increased proportionally with the dose (Fig. 1). The model showed no evidence of a target-mediated drug disposition for ibrutinib and as described by the model equations, ibrutinib pharmacokinetics is linear and does not depend on the dose nor on time.

Finally, we explored the relationship between ibrutinib plasmatic exposure at the M1 visit and discontinuation of ibrutinib therapy 12 months after inclusion. This endpoint is an important surrogate as it has been shown that stopping ibrutinib treatment during the first year of therapy has a negative impact on overall survival and progression-free survival [26]. Patients who had treatment discontinuation for toxicity had higher plasmatic ibrutinib exposure. This association was found to be statistically significant despite the substantial intra-individual variability. No trend was observed in the case of treatment discontinuation for disease progression in patients with CLL. A trend was visible for patients with MCL: patients having disease progression had lower exposure. This result is not statistically significant and is observed in a small number of patients, it should be further investigated. A complete and final PK-PD relationship analysis will be conducted when all patients complete their clinical monitoring. Our PK model could be used to improve adherence to ibrutinib by optimising dosing regimens, especially during the first year of treatment and consequently increase overall survival.

The results we present in this work are useful to assess the relevance of practicing TDM for ibrutinib. To date, no reference levels or TDM recommendations for ibrutinib have been published. Ibrutinib stability at ambient temperature within plasma samples makes TDM practically feasible. Additionally, the model could be used to estimate this daily AUC from a limited number of samples. On the one hand, ibrutinib shows high inter-individual variability and we found no covariate that could be assessed a priori to reduce this variability. Furthermore, higher ibrutinib AUC was found to be associated with the occurrence of adverse drug reactions. Therefore, TDM could be useful to predict which patients are at higher risk of drug-induced toxicity. On the other hand, intra-individual variability is high, which is not in favor of establishing TDM, but this variability could be reduced by better control of food conditions at the moment of drug intake. Regarding these results, the interest in establishing TDM for ibrutinib should be further investigated.

5 Conclusions

This popPK model based on both ibrutinib and DHD-ibrutinb concentrations fits the data well and was validated on an external population. No covariates with a clinically relevant effect on ibrutinib or DHD-inbrutinib exposure were identified. A significant association was found between treatment discontinuation for toxicity and exposure to ibrutinib. This PK-PD relationship concurs with the large inter-individual PK variability of ibrutinib, and was observed despite substantial intra-individual variability. This finding represents a first rationale for TDM of ibrutinib, which the present PK model can help develop and thus improve patients' adherence to ibrutinib and increase response to treatment. Furthermore, this PK model can be used for PK-PD modelling describing lymphocyte dynamics under ibrutinib treatment.

Compliance with Ethical Standards

Funding This study has been supported by the French National Drug Agency (ANSM), the French National Research Agency (ANR, project CAPTOR PHUC-001), and the AVIESAN, INCa and INSERM Plan Cancer program (project C15092BS).

Conflict of interest Loïc Ysebaert received grant support and honorarium fees from Roche, Abbvie, Gilead and Janssen, but not in the scope of the present study. Lucie Obéric received honorarium fees from Roche and Janssen, but not in the scope of the present study. Fanny Gallais, Fabien Despas, Sandra De Barros, Loïc Dupré, Anne Quillet-Mary, Caroline Protin, Fabienne Thomas, Ben Allal, Etienne Chatelut and Mélanie White-Koning have no conflicts of interest that are directly relevant to the content of this article.

Ethics Approval The study was conducted in compliance with ethical standards.

Consent to Participate All patients gave their written informed consent.

References

1. Smith MR. Ibrutinib in B lymphoid malignancies. Expert Opin Pharmacother. 2015;16(12):1879–87.
2. Honigberg LA, Smith AM, Sirisawad M, Verner E, Loury D, Chang B, et al. The Bruton tyrosine kinase inhibitor PCI-32765 blocks B-cell activation and is efficacious in models of autoimmune disease and B-cell malignancy. Proc Natl Acad Sci USA. 2010;107(29):13075–80.
3. Niiro H, Clark EA. Regulation of B-cell fate by antigen-receptor signals. Nat Rev Immunol. 2002;2(12):945–56.
4. Woyach JA, Johnson AJ, Byrd JC. The B-cell receptor signaling pathway as a therapeutic target in CLL. Blood. 2012;120(6):1175–84.
5. Byrd JC, Furman RR, Coutre SE, Flinn IW, Burger JA, Blum KA, et al. Targeting BTK with ibrutinib in relapsed chronic lymphocytic leukemia. N Engl J Med. 2013;369(1):32–42.
6. Ponader S, Chen S-S, Buggy JJ, Balakrishnan K, Gandhi V, Wierda WG, et al. The Bruton tyrosine kinase inhibitor PCI-32765 thwarts chronic lymphocytic leukemia cell survival and tissue homing in vitro and in vivo. Blood. 2012;119(5):1182–9.
7. de Rooij MFM, Kuil A, Geest CR, Eldering E, Chang BY, Buggy JJ, et al. The clinically active BTK inhibitor PCI-32765 targets B-cell receptor- and chemokine-controlled adhesion and migration in chronic lymphocytic leukemia. Blood. 2012;119(11):2590–4.
8. Scheers E, Leclercq L, de Jong J, Bode N, Bockx M, Laenen A, et al. Absorption, metabolism, and excretion of oral ^{14}C radiolabeled ibrutinib: an open-label, phase I, single-dose study in healthy men. Drug Metab Dispos Biol Fate Chem. 2015;43(2):289–97.
9. de Jong J, Skee D, Murphy J, Sukbuntherng J, Hellemans P, Smit J, et al. Effect of CYP3A perpetrators on ibrutinib exposure in healthy participants. Pharmacol Res Perspect. 2015;3(4):e00156.
10. European Medicines Agency. Committee for Medicinal Products for Human Use (CHMP). 24 July 2014, EMA/CHMP/645137/2014. https://www.ema.europa.eu/documents/assessment-report/imbruvica-epar-public-assessment-report_en.pdf. Accessed 11 Mar 2020.
11. Marostica E, Sukbuntherng J, Loury D, de Jong J, de Trixhe XW, Vermeulen A, et al. Population pharmacokinetic model of ibrutinib, a Bruton tyrosine kinase inhibitor, in patients with B cell malignancies. Cancer Chemother Pharmacol. 2015;75(1):111–21.
12. Elens L, van Gelder T, Hesselink DA, Haufroid V, van Schaik RHN. CYP3A4*22: promising newly identified CYP3A4 variant allele for personalizing pharmacotherapy. Pharmacogenomics. 2013;14(1):47–62.
13. Lee S-J, Goldstein JA. Functionally defective or altered CYP3A4 and CYP3A5 single nucleotide polymorphisms and their detection with genotyping tests. Pharmacogenomics. 2005;6(4):357–71.
14. Yates CR, Zhang W, Song P, Li S, Gaber AO, Kotb M, et al. The effect of CYP3A5 and MDR1 polymorphic expression on cyclosporine oral disposition in renal transplant patients. J Clin Pharmacol. 2003;43(6):555–64.
15. Sheiner LB, Beal SL. Some suggestions for measuring predictive performance. J Pharmacokinet Biopharm. 1981;9(4):503–12.
16. Baverel PG, Dubois VFS, Jin CY, Zheng Y, Song X, Jin X, et al. Population pharmacokinetics of durvalumab in cancer patients and association with longitudinal biomarkers of disease status. Clin Pharmacol Ther. 2018;103(4):631–42.
17. Lindauer A, Di Gion P, Kanefendt F, Tomalik-Scharte D, Kinzig M, Rodamer M, et al. Pharmacokinetic/pharmacodynamic modeling of biomarker response to sunitinib in healthy volunteers. Clin Pharmacol Ther. 2010;87(5):601–8.
18. Yu H, van Erp N, Bins S, Mathijssen RHJ, Schellens JHM, Beijnen JH, et al. Development of a pharmacokinetic model to describe the complex pharmacokinetics of pazopanib in cancer patients. Clin Pharmacokinet. 2017;56(3):293–303.
19. ter Heine R, Binkhorst L, de Graan AJM, de Bruijn P, Beijnen JH, Mathijssen RHJ, et al. Population pharmacokinetic modelling to assess the impact of CYP2D6 and CYP3A metabolic phenotypes on the pharmacokinetics of tamoxifen and endoxifen. Br J Clin Pharmacol. 2014;78(3):572–86.
20. Bertrand J, Laffont CM, Mentré F, Chenel M, Comets E. Development of a complex parent-metabolite joint population pharmacokinetic model. AAPS J. 2011;13(3):390–404.
21. Kerbusch T, Wählby U, Milligan PA, Karlsson MO. Population pharmacokinetic modelling of darifenacin and its hydroxylated metabolite using pooled data, incorporating saturable first-pass metabolism, CYP2D6 genotype and formulation-dependent bioavailability. Br J Clin Pharmacol. 2003;56(6):639–52.
22. Chen S-S, Chang BY, Chang S, Tong T, Ham S, Sherry B, et al. BTK inhibition results in impaired CXCR4 chemokine receptor surface expression, signaling and function in chronic lymphocytic leukemia. Leukemia. 2016;30(4):833–43.
23. Cervantes-Gomez F, Kumar Patel V, Bose P, Keating MJ, Gandhi V. Decrease in total protein level of Bruton's tyrosine kinase during ibrutinib therapy in chronic lymphocytic leukemia lymphocytes. Leukemia. 2016;30(8):1803–4.
24. Chen LS, Bose P, Cruz ND, Jiang Y, Wu Q, Thompson PA, et al. A pilot study of lower doses of ibrutinib in patients with chronic lymphocytic leukemia. Blood. 2018;132(21):2249–59.
25. Mato AR, Timlin C, Ujjani C, Skarbnik A, Howlett C, Banerjee R, et al. Comparable outcomes in chronic lymphocytic leukaemia (CLL) patients treated with reduced-dose ibrutinib: results from a multi-centre study. Br J Haematol. 2018;181(2):259–61.
26. Follows GA, Forum UKC. Outcomes of patients post ibrutinib treatment for relapsed/refractory CLL: a UK and Ireland analysis. Hematol Oncol. 2017;35(S2):237–8.

Affiliations

Fanny Gallais[1] · Loïc Ysebaert[1,2] · Fabien Despas[3] · Sandra De Barros[4] · Loïc Dupré[5] · Anne Quillet-Mary[1] · Caroline Protin[2] · Fabienne Thomas[1,6] · Lucie Obéric[2] · Ben Allal[1,6] · Etienne Chatelut[1,6] · Mélanie White-Koning[1]

[1] Cancer Research Center of Toulouse, INSERM, UMR-1037, CNRS ERL5294, Paul Sabatier University, Toulouse, France

[2] Department of Hematology, Institut Universitaire du Cancer de Toulouse-Oncopole, 1 avenue Irène Joliot-Curie, 31059 Toulouse, France

[3] Department of Medical and Clinical Pharmacology, Centre of PharmacoVigilance, Pharmacoepidemiology and Drug Information, INSERM, UMR-1027, Pharmacoepidemiology, Assessment of Drug Utilization and Drug Safety, CIC 1426, Toulouse University Hospital, Toulouse, France

[4] Department of Medical and Clinical Pharmacology, Toulouse University Hospital, Toulouse, France

[5] Center for Pathophysiology of Toulouse Purpan, INSERM UMR1043, CNRS UMR5282, Paul Sabatier University, Toulouse, France

[6] Laboratory of Pharmacology, Institut Claudius Regaud, Institut Universitaire du Cancer de Toulouse-Oncopole, Toulouse, France